Electronic Supplementary Material (ESI) for Soft Matter

Combining Dynamic Monte Carlo with Machine Learning to Study Nanoparticle Translocation

Luiz Fernando Vieira[a,b,c] , Alexandra C. Weinhofer[a], William C. Oltjen[a], Cindy Yu[d], Paulo Roberto de Souza Mendes[b], and Michael J. A. Hore,*‡[a]

[a] *Department of Macromolecular Science & Engineering, Case Western Reserve University, 10900 Euclid Avenue, Cleveland, OH 44106, USA. E-mail: hore@case.edu; Tel: +1 216 368 0793*
[b] *Department of Mechanical Engineering, Pontifícia Universidade Católica do Rio de Janeiro, Rua Marquês de São Vicente 225, Rio de Janeiro, RJ 22451-900, Brazil*
[c]*Instituto Nacional de Tecnologia, Ministry of Science, Technology & Innovation, Av. Venezuela, 82 - Rio de Janeiro, RJ 20081-312, Brazil.*
[d]*Hathaway Brown School, 10600 North Park Blvd., Shaker Heights, OH 44122, USA.*

1 Poisson-Nernst-Planck (PNP) Calculations

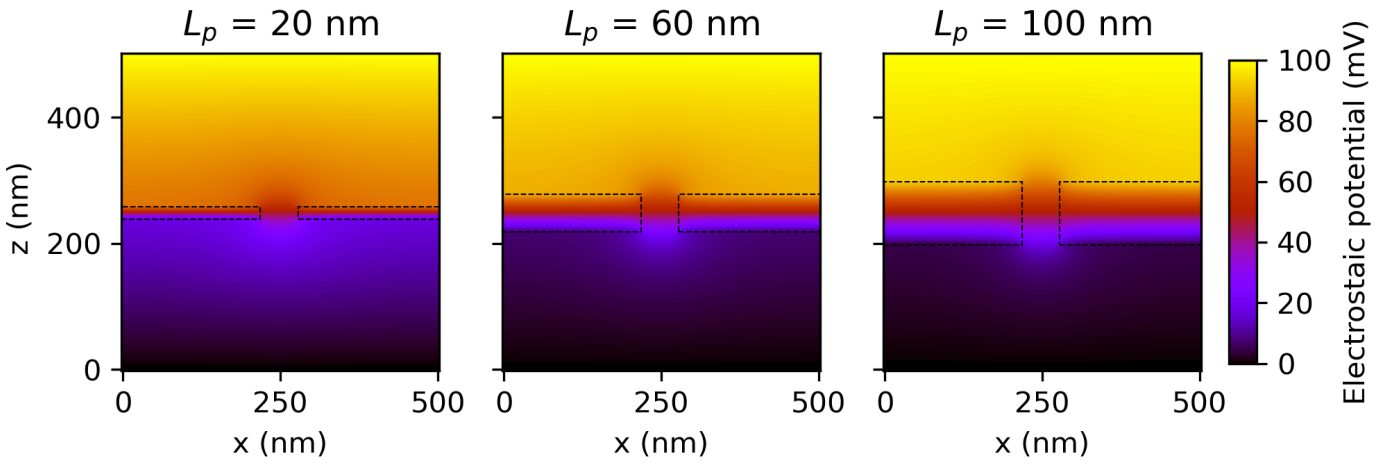

Figure 1 Two dimensional slices in the xz-plane of the electrostatic potential calculated from PNP. The dotted line denotes the position of the membrane, which contains a single nanopore with diameter $d_P = 60$ nm and lengths (left to right) of $L_P = 20$ nm, 60 nm, and 100 nm.

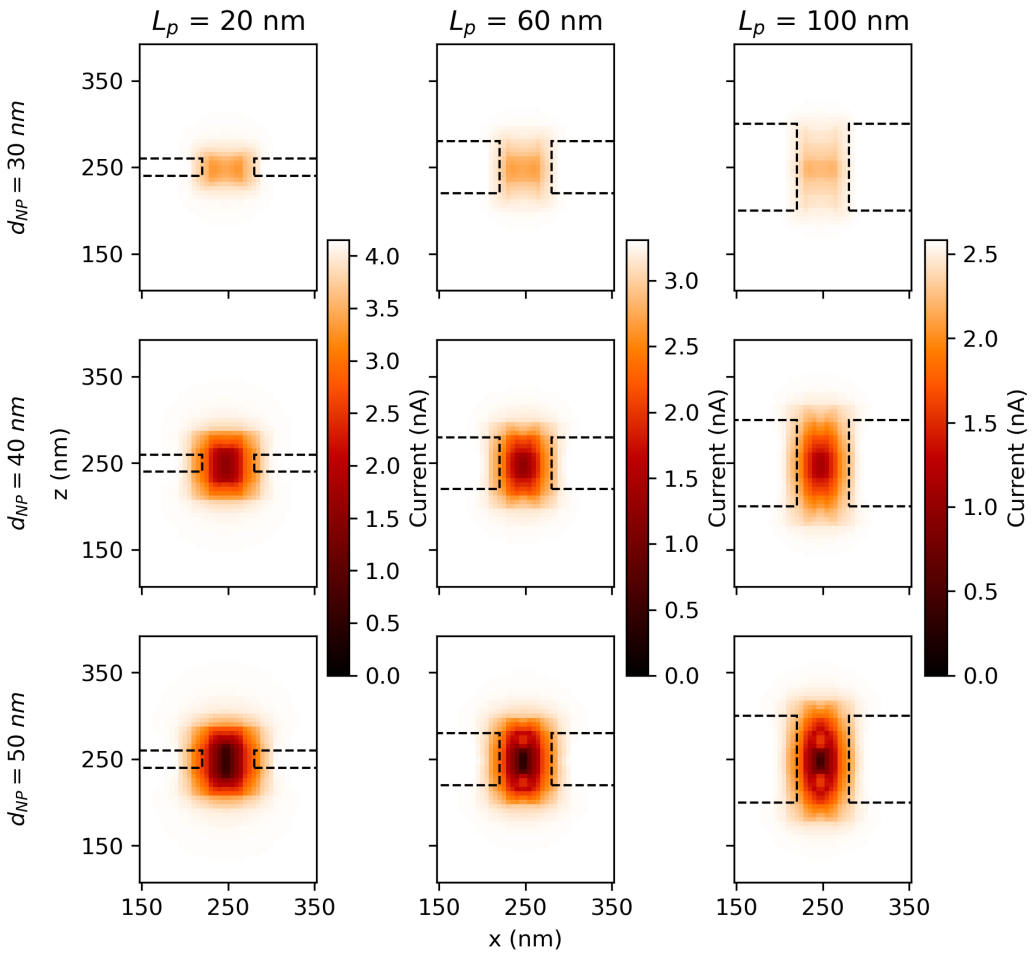

Figure 2 Ionic current through the nanopore for lengths of (left to right) $L_P = 20$ nm, 60 nm, and 100 nm as a function of nanoparticle location. From top to bottom, rows correspond to nanoparticles with diameters $d_{NP} = 30$ nm, 40 nm, and 50 nm. The lowest values of ionic current occur for positions near the central axis of the channel. As the nanoparticle diameter increases, the current decreases as seen in the dark regions in the color map.

2 Neural Network Architecture

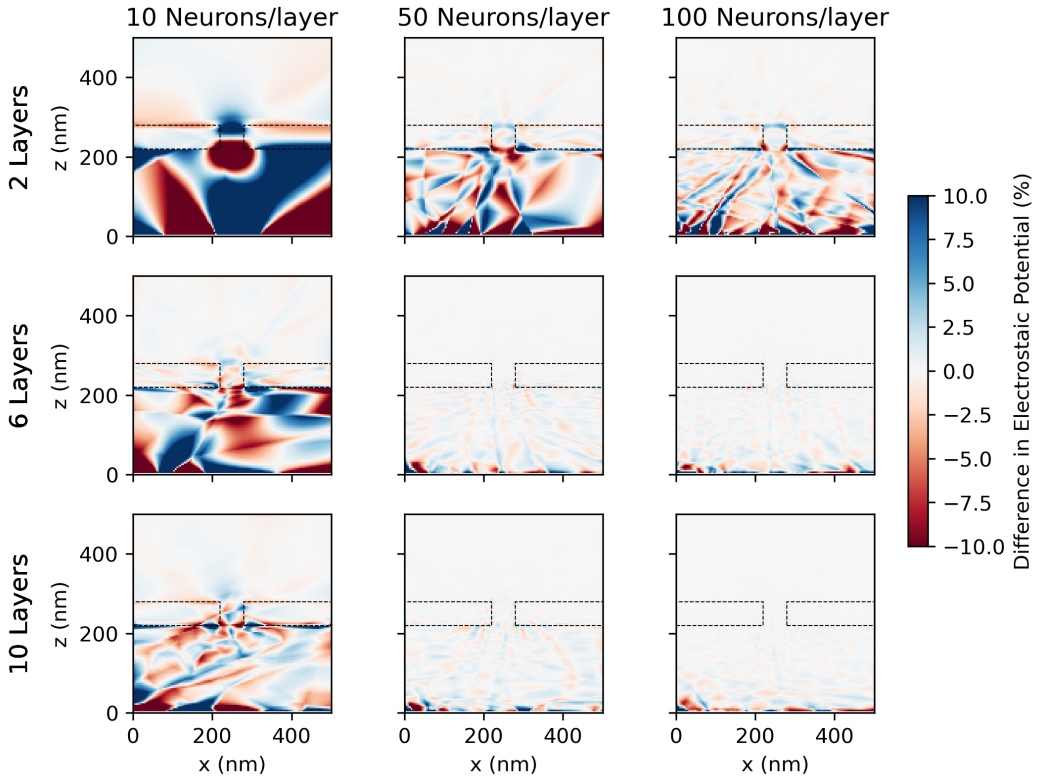

Figure 3 Difference between the electrostatic potential calculated by PNP and predicted by the neural network for a nanopore with diameter $d_P = 60$ nm and length $L_p = 60$ nm for (top to bottom) 2, 6, and 10 layers in the network, and for (left to right) 10, 50 and 100 neutrons per layer. The dashed line denotes the position of the membrane. For all NN configurations, the nanoparticle diameter was fixed at $d_{NP} = 40$ nm. Regions of agreement between PNP calculations and NN predictions are identified by an absence of color.

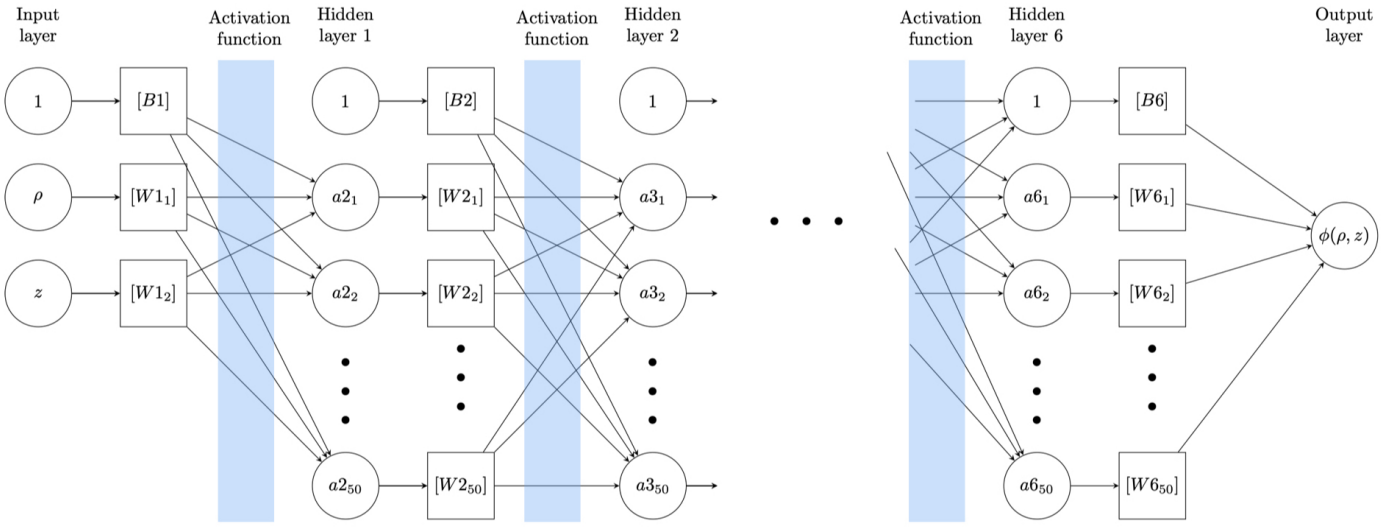

Figure 4 Architecture of the chosen MLP Neural Network. The circles represent the neuron units caring single values in each layer. Each next layer is calculated from the previous layer, where the value in each neuron is modified by a row vector of weights (squares) and an activation function (blue rectangle shade). Neurons with a value equal to 1 were added to each layer allowing to account the effect of the biases and weights as matrix multiplication step, by the concatenation of all row vectors Bi and Wi_j in a single matrix.

3 Analytical Description of Nanoparticle Transport

In a uniform field, analytical expressions of the average transport characteristics can be derived from the probability density function of the metropolis scheme (eq. 6). This can be used to test the code implementation, as well as to compare its results with electrophoretic theory and experimental results. In addition, these expressions can be used to check the sensibility of the results with a given set of simulation parameters.

The total potential energy of a nanoparticle in a uniform electric field is the product of the charge q and the electrostatic potential ϕ:

$$U = q\,\phi \tag{1}$$

The component of the electrostatic field in a given direction is given by the negative of the gradient of the electrostatic potential ϕ:

$$\mathbf{E} = -\nabla\phi \tag{2}$$

These two expressions imply that the potential U of a particle with charge q under an electrostatic field $\mathbf{E}$ which is assumed to be uniform along the x direction (*i.e.*, with the only non-zero component $E_x = E$) can be expressed as:

$$U = -qE\,x \tag{3}$$

where x is the nanoparticle's position in the electric field. In our Monte Carlo simulations, if a trial move consists of a small displacement δx, then the change in potential energy ΔU is:

$$\Delta U = -qE\,\delta x \tag{4}$$

We can also obtain expressions for the mean velocity and electrophoretic mobility of a nanoparticle from similar considerations. The mean velocity $\bar{v}$ is the ratio of the mean displacement $\overline{\delta x}$ and time-step δt

$$\bar{v} = \frac{\overline{\delta x}}{\overline{\delta t}} \tag{5}$$

The (mean) electrophoretic mobility μ_e can be calculated as the ratio of the velocity and the field strength:

$$\mu_e = v/E \tag{6}$$

3.1 Derivation of Acceptance

As stated in Section 2.3 of the main text, the time step used to connect DMC simulations to our experiments is calculated from the intrinsic (MC) time step corrected by the acceptance. To derive an analytical expression of the electrophoretic mobility, it is necessary to derive expressions for the acceptance $\mathscr{A}$ and the mean displacement $\overline{\delta x}$. Acceptance can be derived from the probability distribution function of the trial acceptance (eq. 6) integrated over the interval I:

$$\mathscr{A} = \frac{\int_I p(\Delta U)\,d\Delta U}{\int_I 1\,d\Delta U} \tag{7}$$

where the interval I is defined by the maximum displacement allowed δx_{max}:

$$I = (\Delta U(-\delta x_{max}),\ \Delta U(\delta x_{max})) \tag{8}$$

From eq. 4:

$$\Delta U(\pm\delta x_{max}) = \mp\Delta U_{max} = \mp qE\,\delta x_{max} \tag{9}$$

which leads to the following expressions for the acceptance $\mathscr{A}$:

$$\mathscr{A} = \frac{\int_{\Delta U_{max}}^{-\Delta U_{max}} p(\Delta U)\,d\Delta U}{\int_{-\Delta U_{max}}^{\Delta U_{max}} 1\,d\Delta U} \tag{10}$$

$$\mathscr{A} = 0.5 + \frac{1 - exp(-\beta\Delta U_{max})}{2\beta\Delta U_{max}} \tag{11}$$

3.2 Derivation of Mean Displacement

A schematic of the procedure for obtaining the mean displacement is shown in figure 5. The upper left panel represents probability of accepting the trial move as a function of the change in potential, as defined by the Metropolis scheme. For a positively charged particle in a linearly decreasing electrostatic potential, the electric field points to the positive direction. This implies that all the positive displacements in x are accepted and some of the negative displacement are not, as depicted in the upper right panel of figure 5. In addition, because the position of the rejected trials remains the same, all of the probability density of the rejections (red shaded region) are transferred to zero, as indicated by the arrow.

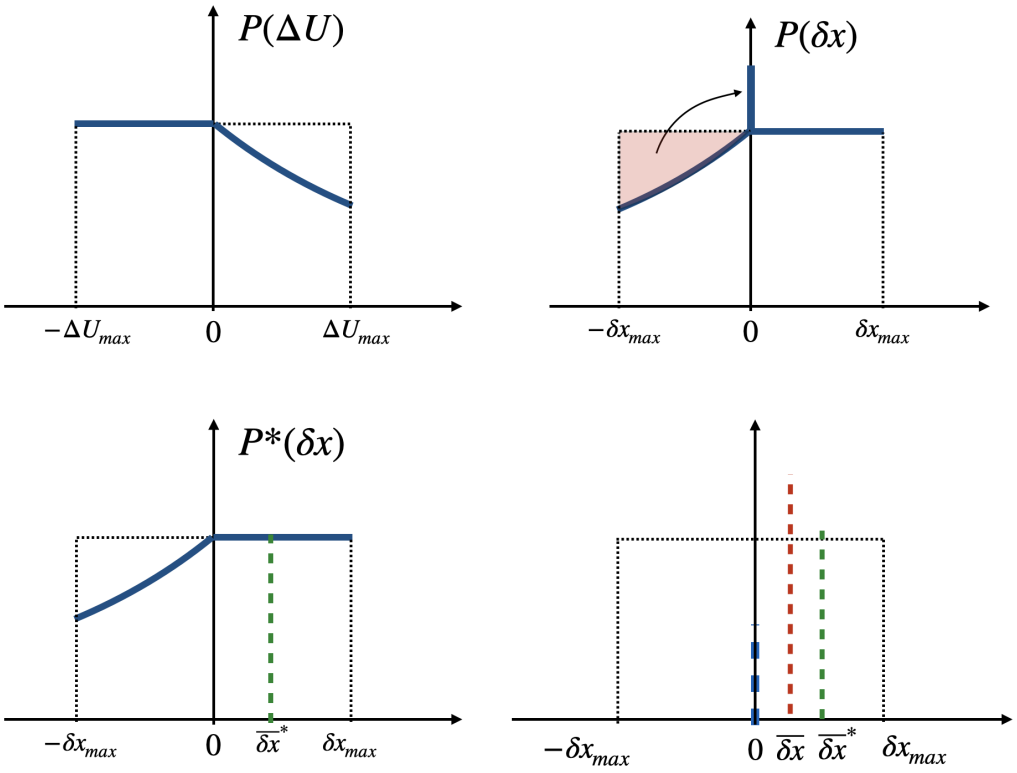

Figure 5 Plots of the probability distributions of (top left) a trial move as a function of the change in the potential energy ΔU, (top right), as a function of the displacement δx, (bottom left) as a function of displacement corrected for rejected moves, and (bottom right) the mean displacements resulting from the use of $P(\delta x)$ and $P^*(\delta x)$.

Since the density of the spike at $\delta x = 0$ is known, it is possible to calculate the mean displacement by calculating the expected value of the distribution without considering the spike (δx^* in the lower left panel of figure 5) and weight-averaging it with the spike for zero displacement (shown in the lower right panel of the figure) as:

$$\overline{\delta x} = \mathscr{A}\,\overline{\delta x}^* + (1-\mathscr{A})\,0 \tag{12}$$

From eq. 4, the mean displacement $\overline{\delta x}$ can be computed from the Metropolis acceptance as:

$$\overline{\delta x} = \frac{\mathscr{A}}{-q\,E}\,\overline{\Delta U} \tag{13}$$

where $\overline{\Delta U}$ is the most probable value for the change in potential energy after a particle's trial move.

We next calculate $\overline{\Delta U}$ from the normalized probability function for U:

$$P(\Delta U) = \frac{p(\Delta U)}{\int_{-\Delta U_{max}}^{\Delta U_{max}} p(\Delta U)\,d\Delta U} \tag{14}$$

$$P(\Delta U) = \frac{p(\Delta U)}{\Delta U_{max} + \frac{1-exp(-\beta \Delta U_{max})}{\beta}} \tag{15}$$

We then calculate $\overline{\Delta U}$ from the probability distribution as:

$$\overline{\Delta U} = \int_{-\Delta U_{max}}^{\Delta U_{max}} \Delta U \; P(\Delta U) \, d\Delta U \tag{16}$$

$$= \frac{1 - exp(-\beta \Delta U_{max})(\beta \Delta U_{max} + 1)}{\beta^2 \Delta U_{max} + \beta - \beta exp(-\beta \Delta U_{max})} - \frac{\Delta U_{max}^2}{2\Delta U_{max} + \frac{2-2exp(-\beta \Delta U_{max})}{\beta}} \tag{17}$$

Finally, the mean displacement then is calculated by substituting equations 10 and 17 in equation 13.

3.3 Comparison with DMC Simulations: Effect of Charge

Figure 6 shows results from our DMC simulations with different values for the net nanoparticle charge. Each colored line represents one of 100 trajectories in the direction x, using $d_{NP} = 30\,\text{nm}, |E| = 1.0\,\text{mV/nm}$ and $\delta x_{max} = 1\,\text{nm}$. The results of acceptance, mean displacement, velocity and mobility from those simulations are compared with the analytical expressions in figure 7, showing an excellent agreement.

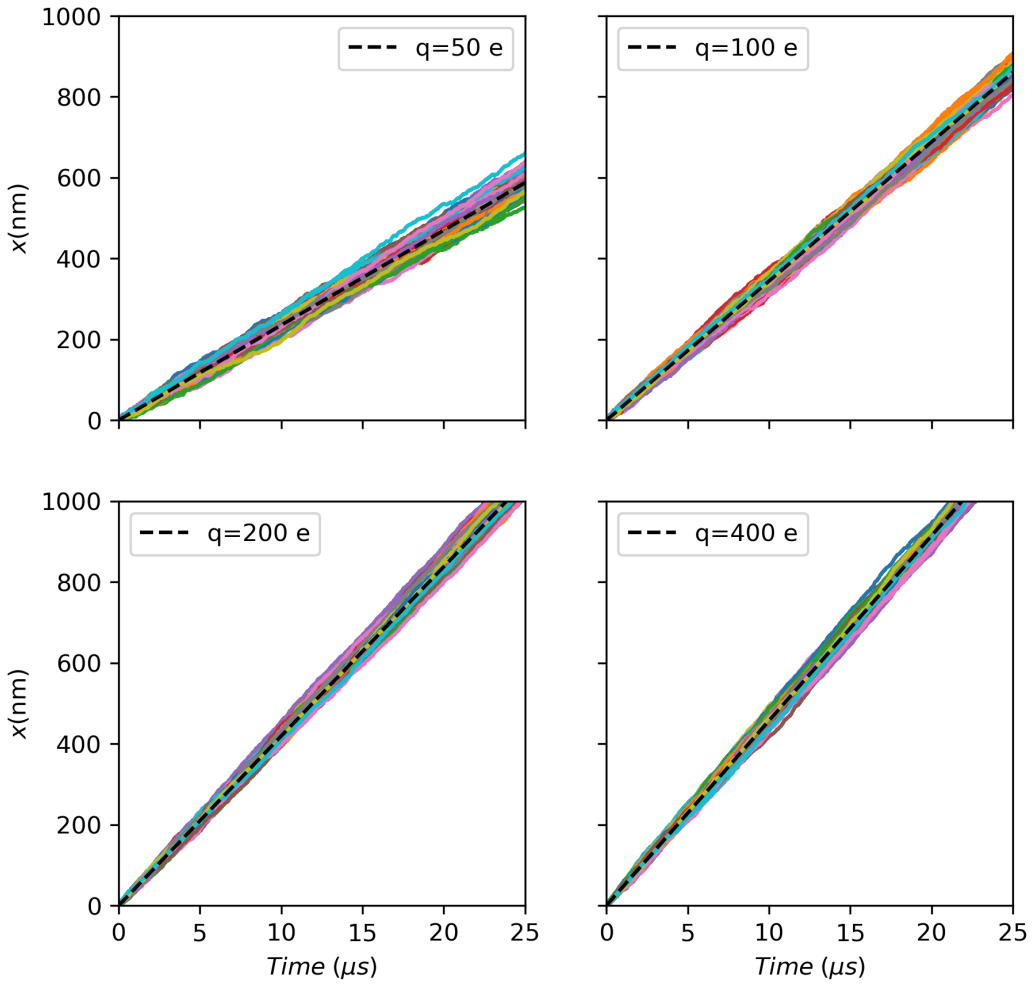

Figure 6 Position as a function of time for 100 trajectories at different values of charge, as noted in the figure legends. The dotted black line indicates the mean position, and its slope the mean velocity.

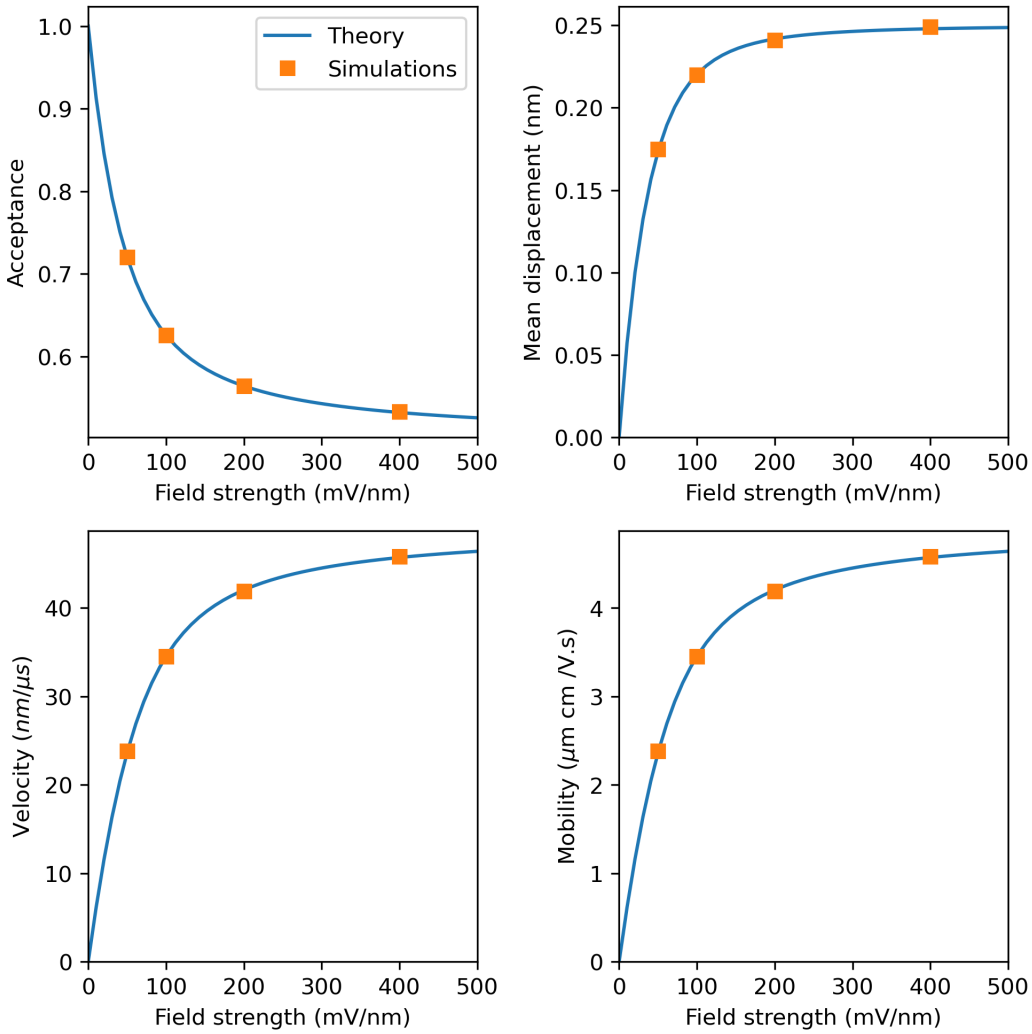

Figure 7 Acceptance, mean displacement, velocity and mobility in function of charge. Points come from DMC simulations, and the lines from the analytical theory outlined above.

The simulations shown above were performed in three dimensions, imposing the electric field only the x direction. Figure 8 shows the squared displacement in the directions not subjected to the field ($\rho^2 = y^2 + z^2$). The recovered diffusion coefficient from the mean squared displacement is very close to the estimates from the Stokes-Einstein equation, and insensitive to the field strength in the x direction, varying only due the inherent variance of the Brownian motion and the finite sampling.

3.3.1 Comparison with Electrophoresis Theory

Electrophoresis theory relates the electrophoretic motion with the properties of the particle, the solution and the electric field. For a non-conductive spherical particle, relations such as the Smoluchowski, Hückel and Henry equations are widely used, and are valid under the assumption of low potential (Zeta potential $\zeta < k_B T/e \approx 25$ mV).

Henry's equation (equation 18) describes the mobility in function of particle permitivity $\varepsilon\varepsilon_o$, zeta potential ζ and solvent viscosity η.

$$\mu_e = \frac{2\varepsilon\varepsilon_0\,\zeta}{3\eta} f(\kappa a) \tag{18}$$

where $f(\kappa a)$ is a function of the Debye–Hückel parameter κ and particle radius a that can be approximated by[1]:

$$f(\kappa a) = \frac{2}{3}\left[1 + \frac{1}{2(1+\frac{2.5}{\kappa a\{1+2\exp(-\kappa a)\}})^3)}\right] \tag{19}$$

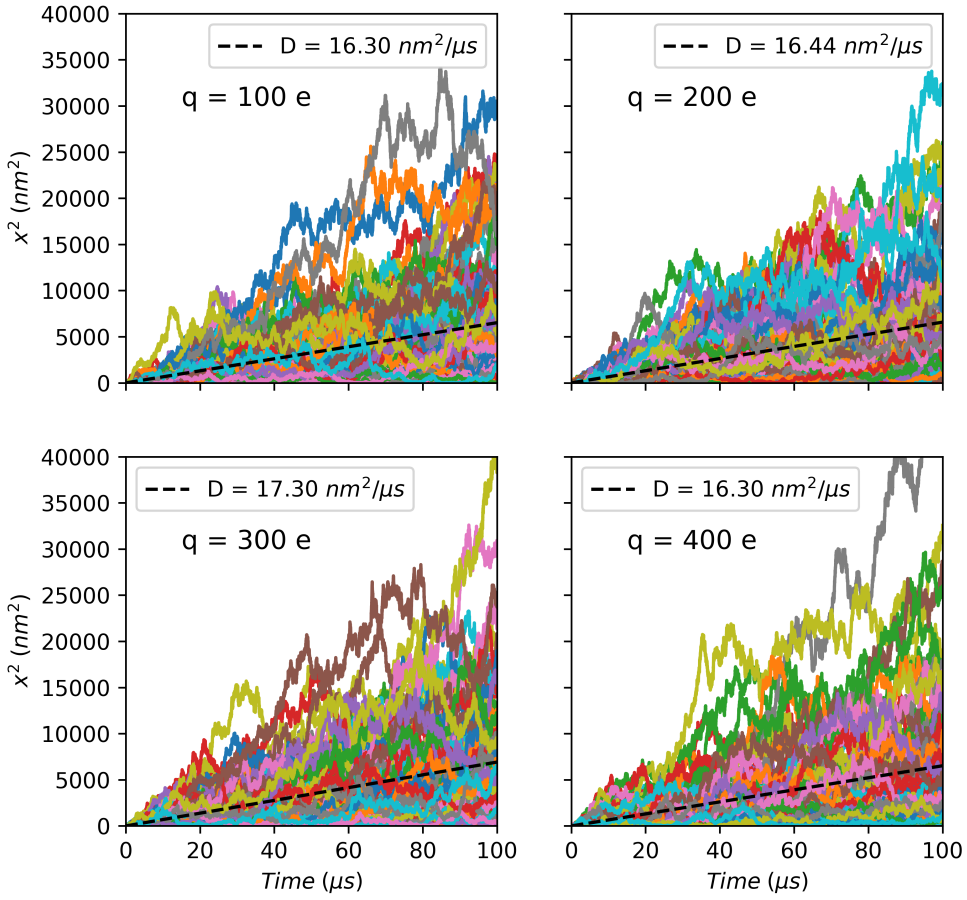

Figure 8 Squared displacement (in y and z directions) as a function of time for 100 particles trajectories. The dashed line denotes the mean-squared displacement, from which the diffusion constant D was calculated. From the Stokes-Einstein equation, we predict $D = 16.34\,\mathrm{nm}^2/\mu\mathrm{s}$.

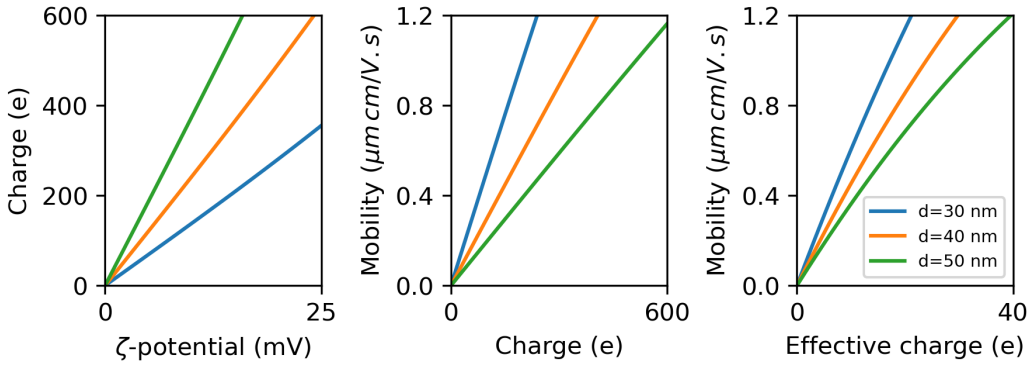

Figure 9 (Left) Charge as a function of ζ potential. (Center) Mobility as a function of charge calculated using electrophoresis theory. (Right) Mobility as a function of charge calculated using the analytical expressions derived for DMC simulations in a uniform electric field. e is the elementary electric charge.

The Debye–Hückel parameter κ, which is the inverse of the Debye length κ^{-1}, is defined as:

$$\kappa = \sqrt{\frac{2N_A e^2 I}{\varepsilon_0 \varepsilon_r k_b T}} \tag{20}$$

Figure 9 shows that influence the electrophoretic motion of nanoparticles in solution. In the left panel, the total surface charge of the nanoparticle, in units of the elementary charge e, is plotted as a function of the ζ potential for three values of particle diameter in an aqueous monovalent salt (e.g. KCl) solution at a concentration of 0.1 mol/L in the low potential regime. The center panel plots the nanoparticle mobility as a function of charge in the low potential regime, with values around $1\mu m.cm/(V.s)$, which are common values observed in experiments. In the right panel, the analytical solution of DMC under a constant electric field of $|E| = 1.0\,\mathrm{mV/nm}$ and $\delta x_{max} = 1\,\mathrm{nm}$ is plotted as a function of the effective charge of the nanoparticle. Comparing middle and rightmost panels, we observe that for same charge, the DMC approach results in mobilities more than 10 times of the predicted by the electrophoresis equations. The simple potential expressed by equation 1 does not take in consideration the drag from solvent and the ionic cloud in the motion of the charged particle. For this reeason, we chose to keep the simple form of the potential (eq. 1) for the simulations and use nonphysical values of charge that result in desired mobility. However, we emphasize that in other measurement techniques, such as dynamic light scattering (DLS), the mobility is the fundamental property of measurement, with the charge or ζ potential calculated from the mobility using electrophoretic theory. Therefore, our DMC simulations impose particular values of the electrophoretic mobility instead of electric charge.

3.3.2 Comparison with DMC Simulations: Effect of Electric Field Strength

The time scaling used in DMC works under the assumption that the acceptance probability does not depend on the step size or direction of the displacement. Although this is never true in a monotonically increasing potential as it used here, it should hold a good approximation in the case of small displacements. Another consequence of this violation is the fact of mobility turns out to be dependent on the field, which is not expected experimentally. However, for the field strength values typically found in the configurations in this study, the variation in the mobility with the field is very low, as is shown in Figure 10.

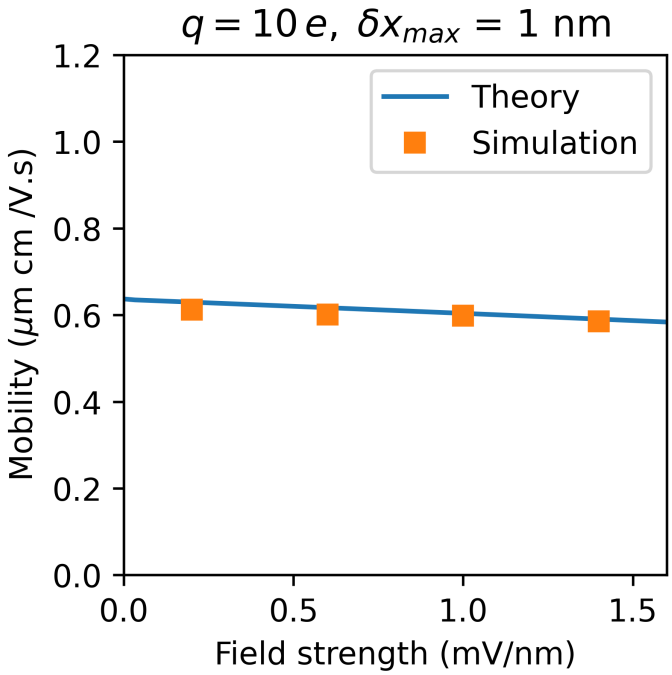

Figure 10 Mobility as a function of field strength for a $d_{NP} = 30$ nm, $q = 10e$, and $\delta x_{max} = 1$ nm.

3.4 Complementary DMC Results

Figure 11, 12 and 13 show 500 overlaid current traces for full translocations in black and collisions in blue. The figures include all three values of nanoparticle diameter, mobility, and nanopore length.

Notes and references

[1] H. Ohshima, *Encyclopedia of Biocolloid and Biointerface Science 2V Set*, John Wiley & Sons, Inc., 2016, pp. 430–438.

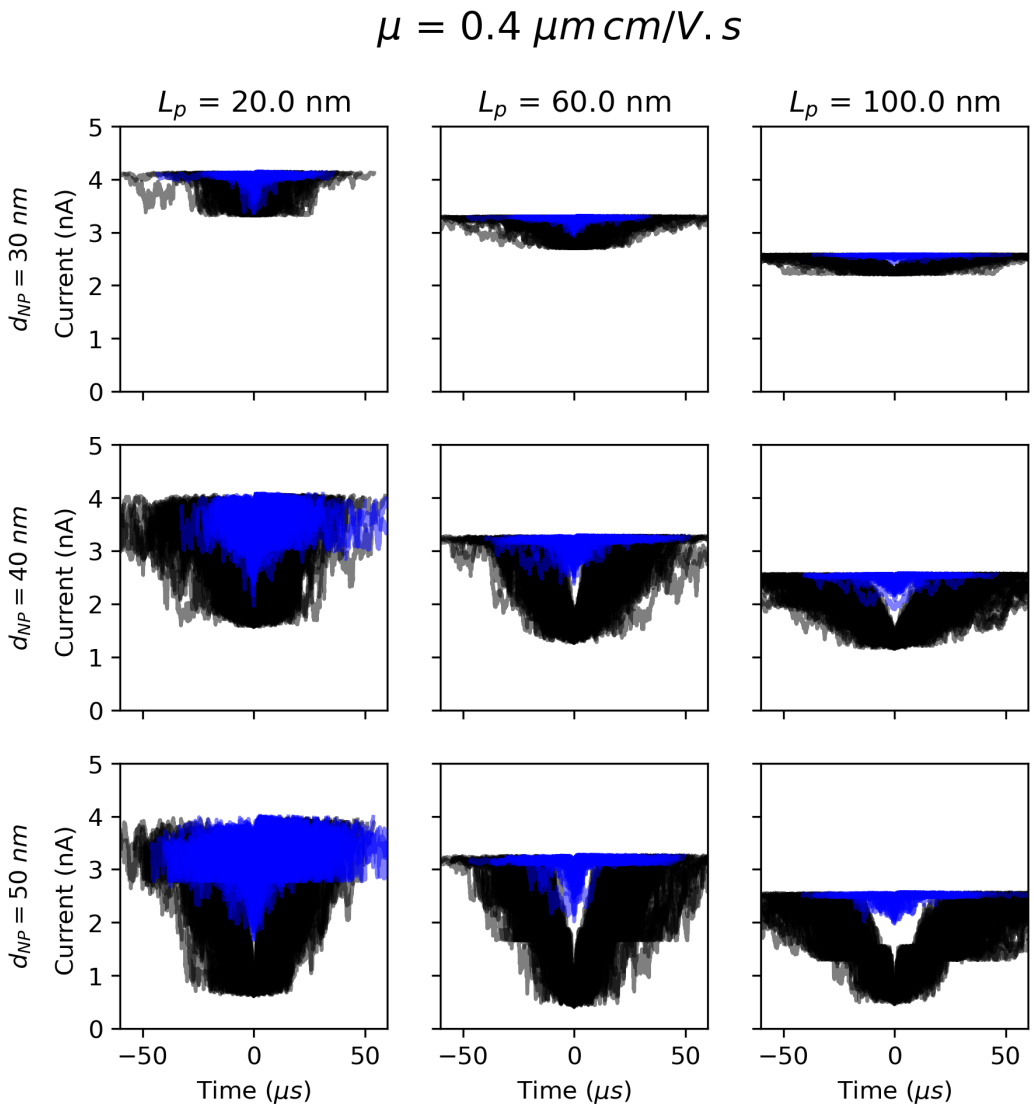

Figure 11 Current as a function of time for 500 overlapped events for a particle mobility of $\mu_{NP} = 0.4\ \mu\mathrm{m.cm/V \cdot s}$ and different conditions of particle diameter (rows) and pore length (columns). Full translocation events are shown in black and collisions in blue.

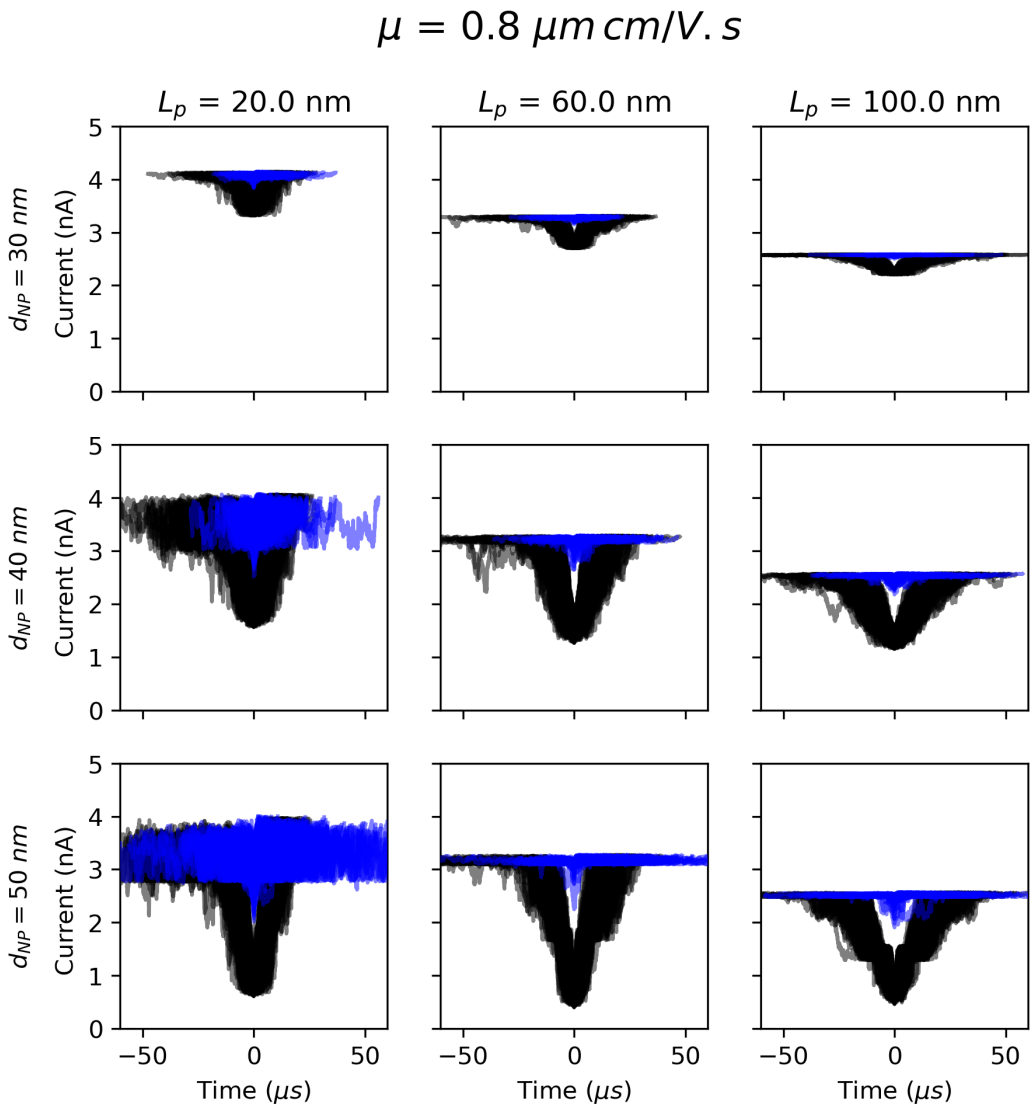

Figure 12 Current as a function of time for 500 overlapped events for a particle mobility of $\mu_{NP} = 0.8\ \mu\mathrm{m.cm/V \cdot s}$ and different conditions of particle diameter (rows) and pore length (columns). Full translocation events are shown in black and collisions in blue.

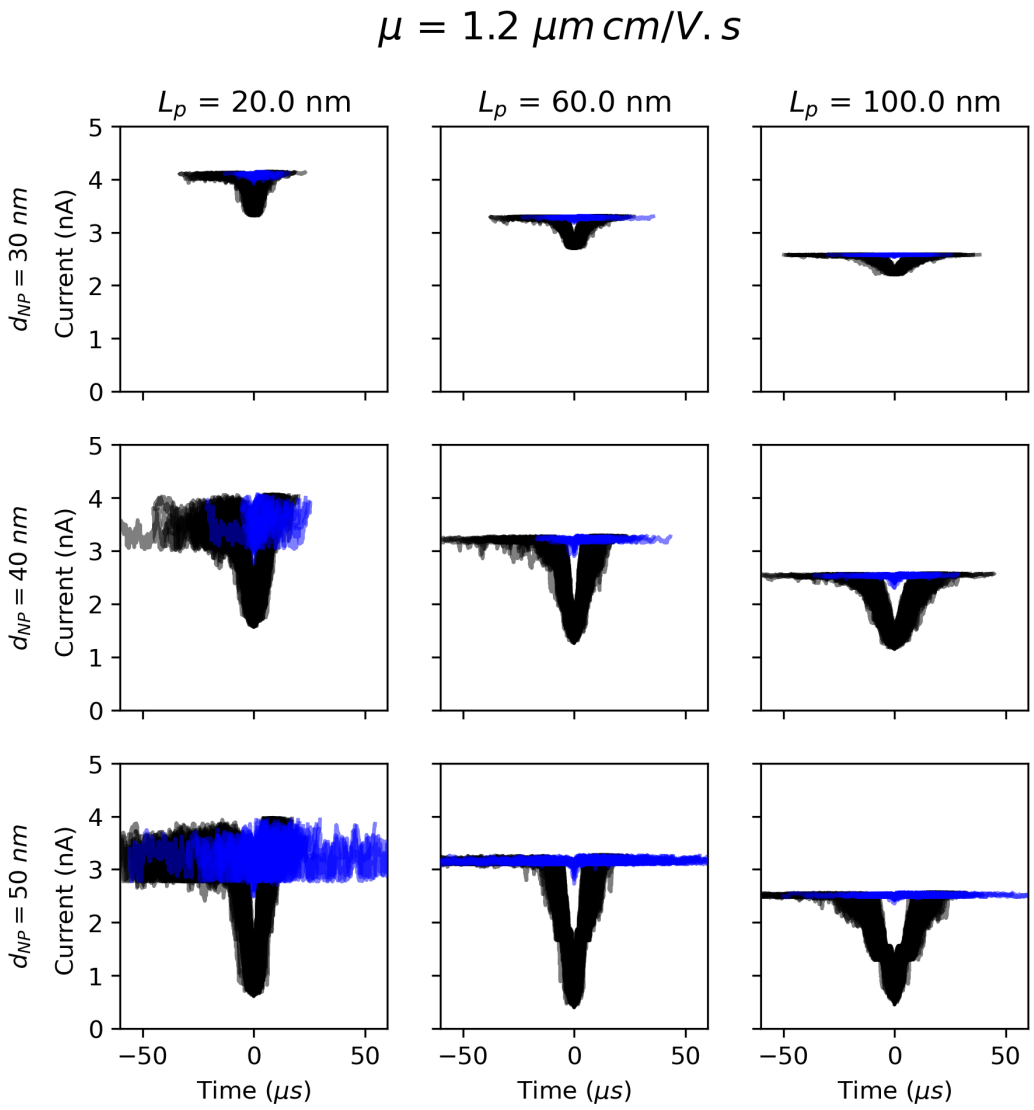

Figure 13 Current as a function of time for 500 overlapped events for a particle mobility of $\mu_{NP} = 1.2\ \mu\mathrm{m.cm/V \cdot s}$ and different conditions of particle diameter (rows) and pore length (columns). Full translocation events are shown in black and collisions in blue.